Journal of Environmental Management 249 (2019) 109210

Contents lists available at ScienceDirect

Journal of Environmental Management

journal homepage: www.elsevier.com/locate/jenvman

Research article

Heat risk assessment for the Brussels capital region under different urban planning and greenhouse gas emission scenarios

Marie-Leen Verdonck[a], Matthias Demuzere[b], Hans Hooyberghs[c], Frederik Priem[d], Frieke Van Coillie[a,*]

[a] Department of Environment University, Gent, Belgium
[b] Department of Geography, Ruhr-University Bochum, Bochum, Germany
[c] Unit Environmental Modelling, Vlaamse Instelling voor Technologisch Onderzoek (VITO), Belgium
[d] Department of Geography, Vrije Universiteit, Brussel, Belgium

ABSTRACT

Urban residents are exposed to higher levels of heat stress in comparison to the rural population. As this phenomenon could be enhanced by both global greenhouse gas emissions (GHG) and urban expansion, urban planners and policymakers should integrate both in their assessment. One way to consider these two concepts is by using urban climate models at a high resolution. In this study, the influence of urban expansion and GHG emission scenarios is evaluated at 100 m spatial resolution for the city of Brussels (Belgium) in the near (2031–2050) and far (2081–2100) future. Two possible urban planning scenarios (translated into local climate zones, LCZs) in combination with two representative concentration pathways (RCPs 4.5 and 8.5) have been implemented in the urban climate model UrbClim. The projections show that the influence of GHG emissions trumps urban planning measures in each period. In the near future, no large differences are seen between the RCP scenarios; in the far future, both heat stress and risk values are twice as large for RCP 8.5 compared to RCP 4.5. Depending on the GHG scenario and the LCZ type, heat stress is projected to increase by a factor of 10 by 2090 compared to the present-day climate and urban planning conditions. The imprint of vulnerability and exposure is clearly visible in the heat risk assessment, leading to very high levels of heat risk, most notably for the North Western part of the Brussels Capital Region. The results demonstrate the need for mitigation and adaptation plans at different policy levels that strive for lower GHG emissions and the development of sustainable urban areas safeguarding livability in cities.

1. Introduction

Expanding urban areas drive global climate change due to greenhouse gas (GHG) emissions and land use change (Ali, 2018; Ali et al., 2018; Benson-Lira et al., 2016; Wouters et al., 2017; Seto et al., 2012). However, this paper focuses on how these climatic changes are expected to adversely influence the urban ecosystem (Revi et al., 2014; Watts et al., 2015). As the world continues to urbanize, global sustainable development challenges and opportunities will increasingly be concentrated in cities, as was already specified by (Djiglav, 2007): “The battle for life on Earth will be won or lost in cities”. In this respect, it is of utmost importance that urban policies address mitigation and adaption to climate change at different scales in order to guarantee the livability of cities in the future (Ali et al., 2017; Bramley and Power, 2009; Mills, 2007; Wouters et al., 2017).

In order for policy to be effective, climate knowledge should be incorporated into urban decision-making as a component for future urban planning and in the development of smart cities. Generally, this is done using climate models. In recent years, many studies focused on improving the representation of urban surfaces in these models to simulate realistic urban temperatures. This work is highly relevant as cities are already suffering from higher temperatures due to the urban heat island (UHI) effect and will be more vulnerable to extreme heat stress under future climate projections (IPCC, 2012). Recent studies indicate that urban and rural areas respond similarly to climate change, but urban areas are more prone to suffer from extreme heat (Fischer et al., 2012; Oleson et al., 2018). Global climate models are typically run at a coarse resolution, thus, inhibiting the analysis of the intra-urban effects of heat stress-related problems at the neighborhood scale. Therefore, regional climate models with higher resolutions are needed (Argüeso et al., 2015; Kendon et al., 2017). Since downscaling is computationally very expensive, only a limited amount of GHG and land use change scenarios are usually used (Kendon et al., 2017). A recent study by Wouters et al. (2017) combined a business-as-usual (BAU) urban growth scenario and three global GHG emissions scenarios to evaluate future heat stress in Belgium (White and Engelen, 2000). Results show that the influence of the global emission scenarios trumps the local land use change input in terms of overall heat stress at the

* Corresponding author. Coupure 653, B-9000, Gent, Belgium.
E-mail addresses: marieleen.verdonck@ugent.be (M.-L. Verdonck), Matthias.demuzere@rub.de (M. Demuzere), hans.hooyberghs@vito.be (H. Hooyberghs), fpriem@vub.ac.be (F. Priem), frieke.vancoillie@ugent.be (F. Van Coillie).

https://doi.org/10.1016/j.jenvman.2019.06.111
Received 4 July 2018; Received in revised form 16 June 2019; Accepted 24 June 2019

2.8 km scale. Future heat stress has a strong spatial variation, similar to current heat stress. Remarkably, the worst GHG emissions scenarios anticipate that the rural heat stress during the coldest years will exceed the urban heat stress in the warmest years in the present day.

Even high-resolution regional climate models, simulating climate characteristics at a regional scale (> 1 km) as used by Wouters at al. (2017), have a resolution that is too coarse to capture the intra-urban heterogeneity often present as neighborhood scales. As such, a higher horizontal spatial resolution (1 km or higher) is required to evaluate structural changes in terms of urban planning. Urban climate models at the neighborhood scale can play a vital role in the evaluation of different urban planning scenarios (Eliasson, 2000; Hebbert and Mackillop, 2013; Mills, 2007). It seems, however, that researchers and urban planners are facing a "knowledge circulation failure", due to a mismatch between urban climate knowledge and planning concerns (Hebbert and Mackillop, 2013). To overcome this gap, existing and future research should be aligned for planning use and to meet urban planning needs (Alcoforado et al., 2009; Gál et al., 2009; Mills et al., 2010). Urban growth scenarios as a component of a planning support system are thus a valuable tool for exploring the spatial impact of decisions on future urban planning and can be important to test the impact of different visions on spatial design (Van De Voorde et al., 2016).

In this study, the UrbClim model (De Ridder et al., 2015) is run at a spatial resolution of 100 m for Brussels (Belgium). The high resolution has an important benefit when assessing the heat exposure of urban residents on a neighborhood level. Two different scenarios for urban planning are combined with global GHG emissions scenarios (representative concentration pathways (RCP) 4.5 and 8.5) to evaluate the impact of both urban planning, in terms of Local Climate Zones (LCZ) (cfr. Alexander et al. (2016)), and GHG emissions for the near and far future. Local climate zones are formally defined as "regions of uniform surface cover, structure, material, and human activity that span hundreds of meters to several kilometers in horizontal scale" (Stewart and Oke, 2012). The scheme consists of 17 standard zones, with a unique air temperature regime at screen height (1–2 m above the ground) and in similar atmospheric and surface relief conditions (Stewart et al., 2014) (Fig. 1).

Verdonck et al. (2018) already indicated a significant difference between the thermal behavior of each zone and the potential of LCZ maps as a heat stress indicator under present-day climate conditions. Yet in this study, the maps are used to assess future heat risk in function of urban planning measures and global GHG emissions scenarios for the Brussels Capital Region, thereby targeting two research questions:

- How does the LCZ map for Brussels translate to LCZ maps based on two urban planning scenarios (UPS)?
- How do GHG and urban planning scenarios influence heat risk in the Brussels Capital Region?

2. Methodology and methods

First, in order to develop two different urban planning scenarios, the LCZ map for Brussels, which was developed in Verdonck et al. (2017), is translated to statistical sectors and is used as a base for the two urban

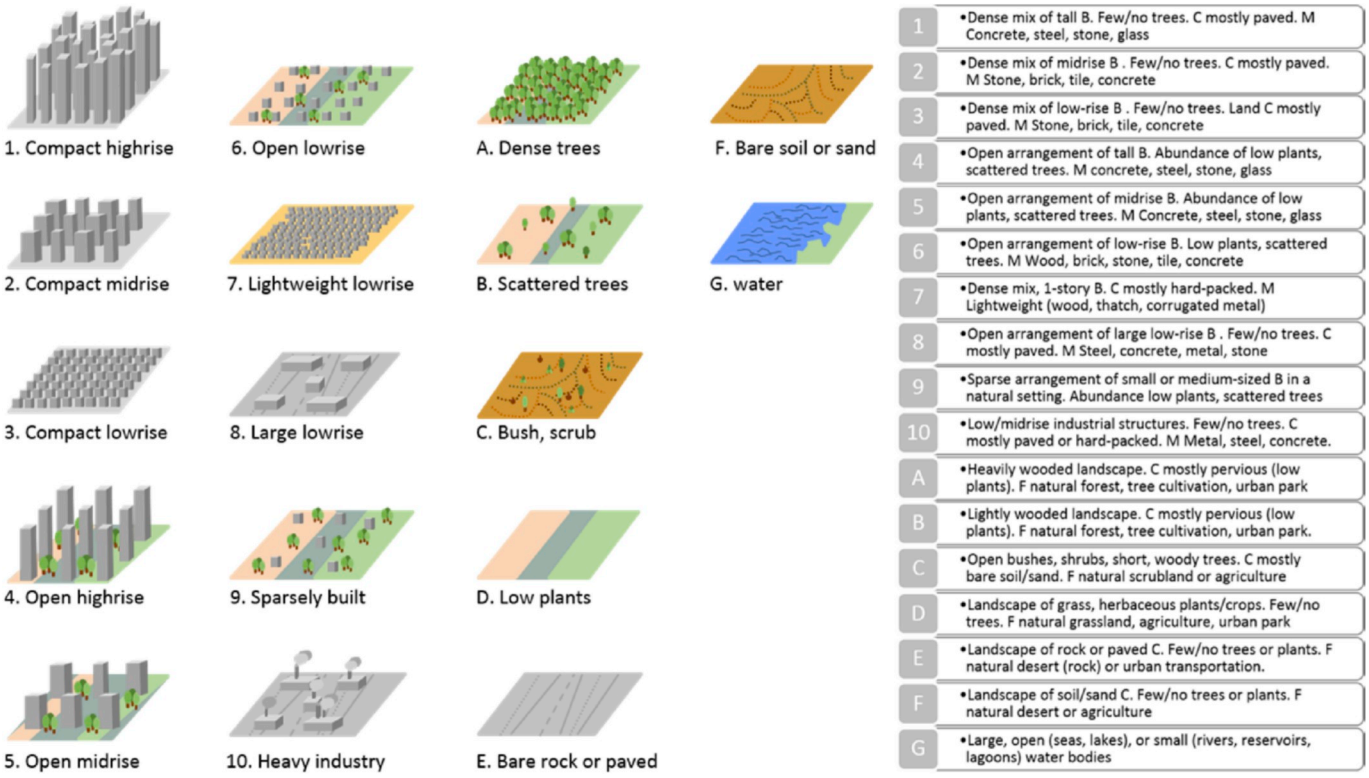

Fig. 1. Urban (1–10) and natural (A–G) LCZ types and their characteristics (adapted from Table 2 in Stewart and Oke (2012), text shortened, icons reworked) B: Buildings; C: cover; M: materials; F: function; Tall: > 10 stories, Midrise: 3–9 stories, Low: 1–3 stories (Adapted from Stewart and Oke (2012)).

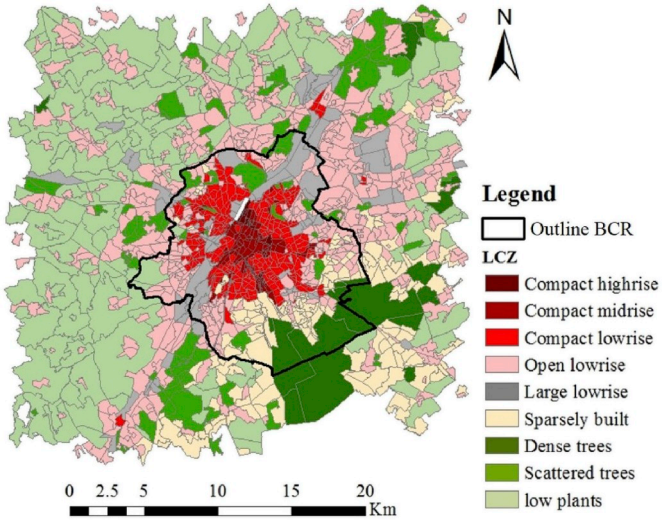

Fig. 2. Present-day LCZ map for Brussels using statistical sectors as a mapping unit. The central white area coincides with the canal zone in Brussels which is not located in a statistical sector.

planning scenarios. Statistical sectors are a spatial unit that is finer than that of cities or municipalities and are the smallest spatial unit in Belgium for which census data are made publicly available (ESPON, 2013). Thus, within one municipality multiple statistical sectors exist. Based on the two urban planning scenarios, air temperature is simulated by UrbClim for a reference, a near future (2031–2050, referred to as 2040) and a far future period (2081–2100, referred to as 2090). For the future simulations, two RCP scenarios (RCP 4.5 and RCP 8.5) are taken into account (Section 2.2). Finally, heat stress is assessed for all scenarios in Brussels and a heat risk map for the Brussels Capital Region (outlined in Fig. 2) is presented based on hazard, exposure, and vulnerability, see Section 2.3.

2.1. Relating urban planning scenarios to LCZs

For each statistical sector in Brussels, the majority LCZ (Verdonck et al., 2017) is retained, providing a new LCZ map (Fig. 2).

From this present-day LCZ map, two urban planning scenarios (UPS) are derived:

- The first scenario is based on a BAU approach. Projections by (Poelmans, 2010) show that in this scenario over 40% of the open space in Flanders will be locked and will no longer be accessible by the public by 2050.
- A second scenario integrates the Flemish and Brussels policy direction for 2050. In this sustainable (SUS) scenario, by 2040 no more open space is consumed and the existing built surface is densified and concentrated around major mobility networks.

To define future LCZ maps we used the map in Fig. 2, in combination with a location choice model (Somers et al., 2017). This model is based on a decision tree with a rule set for each scenario (Fig. S1), which simulates where people will live in the future, taking population growth into account. The model generates the new population density, depending on the UPS, at the scale of a statistical sector. Based on the population densities for each LCZ, calculated from the present-day LCZ map (Fig. S2), the population densities for both scenarios are translated into two LCZ maps. Based on the population density values, transition rules for both scenarios are set (Table 1, between squared brackets). These rules are implemented in all statistical sectors. The logic behind the transition rules is closely linked to the logic of the UPS. For example, in the BAU scenario, LCZ 9 (sparsely built) transitions first into LCZ 6 (open lowrise) and only afterward in LCZ 3 (compact lowrise) instead of transitioning into a high-density structure immediately which would happen in SUS. Similarly, for SUS it is possible for LCZ 8 (large lowrise or industrial) to transition into LCZ 5 (open midrise), which translates often in the conversion from old industrial buildings into a newly developed site.

This first rule set delivered two preliminary maps. Since the vision for Flanders and Brussels (Ruimte Vlaanderen, 2016) focuses on densification of the urban centers, optimal use of mobility networks, the introduction of green and blue corridors reaching into the city center and no more consumption of public space after 2040, some additional rules have been implemented for the sustainable scenario:

- Introduction or expansion of green zones (LCZ B) in the Brussels Capital Region (population was compensated in neighboring zones);
- Densification of the satellite villages and towns: All centers are converted to compact lowrise (LCZ 3);
- Transformation of commercial zones on the East–West axis to different built zones based on the Canal plan (Chemetoff, 2014).

2.2. Urban climate projections methodology

Projections for the future climate in Brussels have been obtained by combining the UrbClim model with statistical techniques. The UrbClim model has been extensively validated for the city of Brussels and is suitable to simulate temperatures in the framework of this study (De Ridder et al., 2015). To simulate the future climate, two effects are

Table 2
Explanation of the scenario names for all 10 scenarios.

	Period	RCP	Name
Business-as-usual	Reference period	No RCP	BAU_ref
Business-as-usual	2031–2050	RCP 4.5	BAU_2040_RCP4.5
Business-as-usual	2031–2050	RCP 8.5	BAU_2040_RCP8.5
Business-as-usual	2081–2100	RCP 4.5	BAU_2090_RCP4.5
Business-as-usual	2081–2100	RCP 8.5	BAU_2090_RCP8.5
Sustainable	Reference period	No RCP	SUS_ref
Sustainable	2031–2050	RCP 4.5	SUS_2040_RCP4.5
Sustainable	2031–2050	RCP 8.5	SUS_2040_RCP8.5
Sustainable	2081–2100	RCP 4.5	SUS_2090_RCP4.5
Sustainable	2081–2100	RCP 8.5	SUS_2090_RCP8.5

Table 1
Transition rules for each scenario, population density thresholds (population/km^2) between square brackets.

Business-as-usual (BAU)	Sustainable (SUS)
natural zones = > sparsely built [100]	no conversion from natural to built zones
open lowrise = > compact lowrise [4904]	open low-rise = > open midrise [4904]
sparsely built = > open lowrise [3266]	sparsely built = > open lowrise [3266]
compact lowrise = > compact midrise [6000]	compact lowrise = > compact midrise [6000]
	large open low-rise = > open midrise [4000]

Table 3
Selected vulnerability indicators and supporting data.

Vulnerable group	Supporting data (BISA, 2018; Somers et al., 2017)
Elderly (E)	
	percentage of people older than 65 years
	percentage of people older than 80 years
	percentage of people older than 65 years, living alone
Children (C)	
	percentage of children under the age of 3 years
Population density (P)	
	population density per km^2 (BAU)
	population density per km^2 (SUS)
Income level (I)	
	Average yearly income
	percentage of people who are unemployed for a long time
	percentage social housing

taken into account: urban planning scenarios and GHG emission scenarios. The effects are implemented in a two-step procedure, wherein, first, the land use change due to urban growth is included based on the UPS, and only thereafter the GHG emissions are added to the urban planning results. A detailed description of the implementation can be found in Appendix S3.

In total, 10 different scenarios (Table 2) are assessed. The name for each scenario is based on three components: the urban planning scenario, the time period for which the scenario is run, and the representative concentration pathway.

2.3. Heat risk analysis in function of LCZs

Following (Buscail et al., 2012; Tomlinson et al., 2011), the risk assessment theory focusing on the "Crichton's Risk Triangle" is used, stating that risk is a function of hazard, exposure, and vulnerability (Crichton, 1999). Risk is defined between 0 and 1 and has no unit. When any of the three components is zero, there is no risk.

2.3.1. Hazard

Hazard is something that may cause a risk. There are different hazard types, which can be natural or man-made. The hazard in this study is related to extreme temperatures which can lead to heat stress situations in urban areas. As was described in Verdonck et al. (2018), not only high daytime temperatures are important for heat stress, but also the nighttime cooling rates should be considered. The heatwave degree days (HWDD) (Wouters et al., 2017) take both into account and are used to provide information on hazard in this manuscript for three different periods in time: the reference period, 2040, and 2090. HWDD are defined using the following equation:

$$HWDD = \sum_{k} [(T_{min,k} - 18.2°C)^{+} + (T_{max,k} - 29.6°C)^{+}]h_k$$

This index calculates the sum of exceedance of minimum and maximum thresholds during a heatwave day ($h_k = 1$). The intensity of the heatwaves is taken into account with the concept of exceeding values of those temperature thresholds. The plus sign, $(\ )^{+}$, indicates that only positive values are taken into account. Note that this index is operationally used by Belgian governmental agencies on environment and health to monitor the potential effect of heat stress episodes, as a part of the state of the environment reporting in Flanders (see Brouwers et al., 2015; http://www.milieurapport.be).

2.3.2. Exposure and vulnerability

The exposure component represents what is exposed to the hazard (Tomlinson et al., 2011); in this case, the location of people or activities that can be affected by heat stress (WMO and WHO, 2015). In general, the urban population would be exposed to higher temperatures compared to the rural surroundings, due to the UHI effect. However, Verdonck et al. (2018) show that within a city exposure to high temperatures or heat stress can also depend on the urban morphology. For this reason, population density is often used to account for exposure in

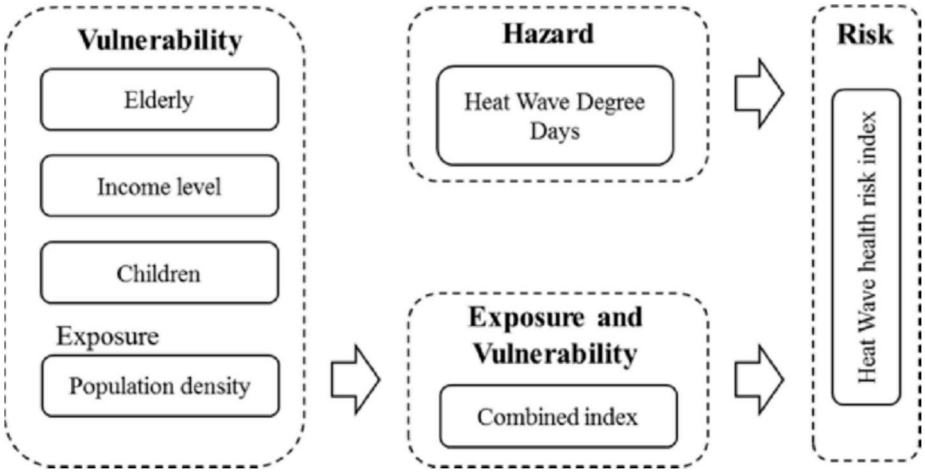

Fig. 3. Flowchart of the integrated spatial heat health risk assessment.

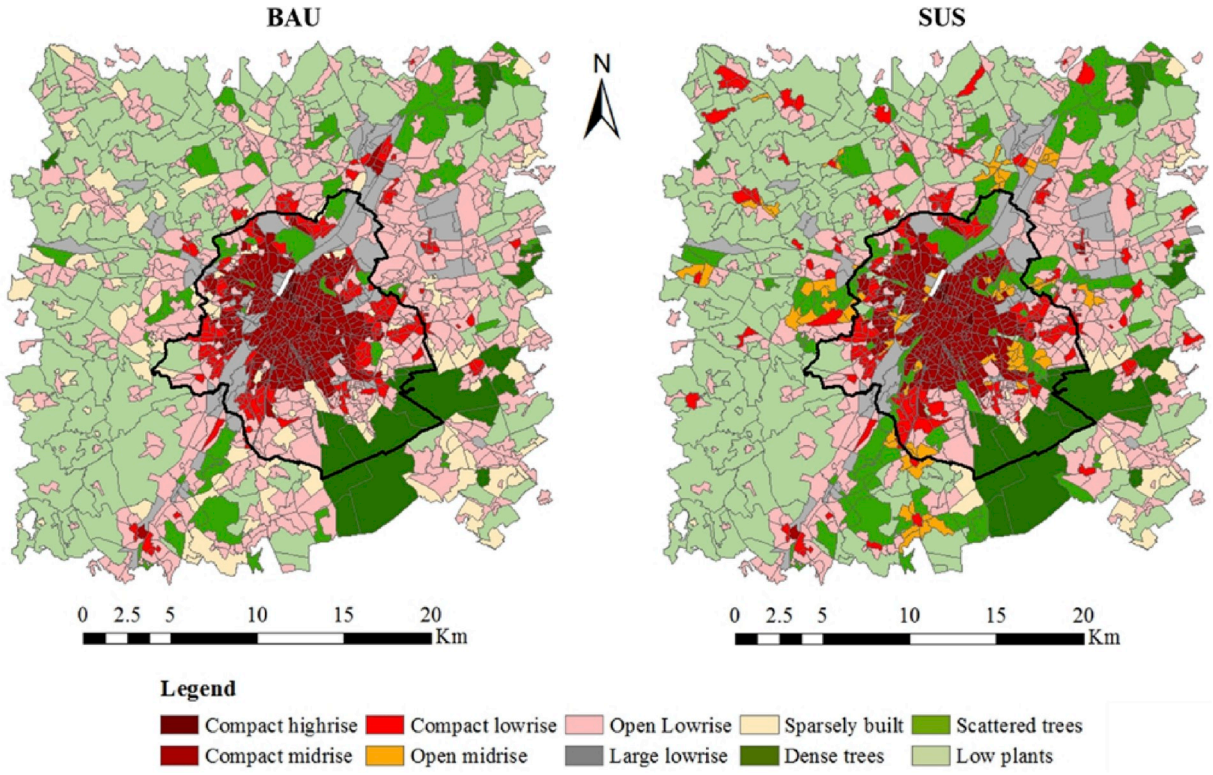

Fig. 4. LCZ map for Brussels using statistical sectors as a mapping unit: business-as-usual (left) and sustainable (right), the Brussels Capital Region is outlined in black.

heat risk studies (Gadeyne, 2016). Since high population densities often correspond to regions with high urban densities and, thus, high UHI intensities (Loughnan et al., 2012), some authors consider exposure to be a part of vulnerability (Scherer et al., 2013). In this study, the same approach is followed and population density is included in the vulnerability index.

Vulnerability can be described as "the characteristics of a person or group and their situation that influences their capacity to anticipate, cope with, resist and recover from the impact of a natural hazard" (Wisner et al., 2003). Multiple studies have reported that some population groups are more susceptible to suffer from heat stress during extreme heat events (Buscail et al., 2012; Dolney and Sheridan, 2006; Hajat et al., 2007; Hajat and Kosatky, 2010; Harlan et al., 2006; Kovats and Kristie, 2006; Lemonsu et al., 2015; Loughnan et al., 2012; Luber and McGeehin, 2008; Morabito et al., 2015; Scheraga and Grambsch, 1998; Tomlinson et al., 2011; Vandentorren et al., 2006): elderly, young children, people with chronic diseases or disabilities, people who are socially isolated, some ethnic groups, economically disadvantaged people, migrant groups, but also people that perform physical activities outdoors or in non-cooled indoor environments. Here four different vulnerability groups are included in the heat risk assessment (Table 3) together with their supporting data layers from (BISA, 2018) at the neighborhood level. Population density is based on the output from the urban dynamics model (Section 2.1) and is available at the spatial scale of the statistical unit, a more detailed scale compared to the neighborhood scale for the other layers.

The vulnerability index, further referred to as the combined index (V), is the equal-weighted linear sum of the four sub-indicators following (Tomlinson et al., 2011): $V = (E + C + P + I)/4$, where E, C, P and I respectively refer to the elderly, children, population density, and income level. In order to compare and combine all indicators, they are normalized to 0–1 using a linear normalization algorithm:

$$\frac{Indicator\ value - min(indicator\ value\ range)}{max(indicator\ value\ range) - min(indicator\ value\ range)}$$

To calculate the indicators "elderly" and "income level" the same method is applied using the different supporting data layers from Table 3.

2.3.3. Risk

Risk is defined as "the probability of future damage and losses to the impact of a given hazard event on an element at risk over a specified time period" (Kervyn, 2015). As shown in Fig. 3, the combined index (exposure and vulnerability) is multiplied with the normalized hazard index to deliver a heatwave health risk (IPCC, 2012):

$$Heat\ risk = V \times normalized\ HWDD$$

The normalized hazard index is calculated based on the minimum hazard (reference period) and the maximum hazard (RCP 8.5 in the far future) over different time periods and RCP scenarios:

$$\frac{Hazard\ value - min(Hazard\ value)}{max(Hazard\ value) - min(Hazard\ value)}$$

Since the supporting census data is only available for the Brussels Capital Region, the heatwave health risk index is only calculated for the Brussels Capital Region and not for the whole extent of the LCZ map (Fig. 2). Readers should also be aware that the combined index is not projected into the future due to lack of data, this might lead to an underestimation of the potential heat risk.

Table 4
Difference in surface area (Km^2 and %) for all zones in the two UPS compared to the present-day situation.

	Built zones (BZ)								Natural zones (NZ)			
	LCZ 1	LCZ 2	LCZ 3	LCZ 5	LCZ 6	LCZ 8	LCZ 9	Total BZ	LCZ A	LCZ B	LCZ D	Total NZ
BAU												
Km^2	0	39.4	−9.6	0	21.1	0.2	−16.9	34.2	0.3	−12.5	−22	−34.2
%	0	4.3	−1.1	0	2.3	0	−1.9	3.8	0	−1.4	−2.4	−3.8
SUS												
Km^2	−0.4	37.9	3.6	23.8	−25.6	−3.5	−63.1	−27.3	0.3	16.7	12.7	27.3
%	0	4.2	0.4	2.6	−2.8	−0.4	−6.9	−3	0	1.8	1.1	3

3. Results

3.1. Relating urban planning scenarios to LCZs

In Fig. 4, the LCZ maps for the BAU and the SUS scenarios are presented and in Table 4, the difference in surface areas for each LCZ is listed for the two scenarios compared to the present-day situation. Both maps indicate clear densification of the Brussels Capital Region by 2040 in comparison to the present-day map (Fig. 2). Almost all compact lowrise zones (LCZ 3) are converted to compact midrise (LCZ 2), resulting in an increase of almost 40 km^2 for both urban planning scenarios, making compact midrise the main built zone in the Brussels Capital Region.

Second, in the SUS scenario, five green corridors (North, North-East, East, South-West, and West of the center), or ventilation axes, are introduced. These corridors provide the urban population with a gateway to the rural surroundings of the Brussels capital. Due to the densification and the implementation of green areas in the SUS scenario, the lowest fraction of built zones can be found here. Moreover, the total amount of built zones decreased by 27.3 km^2 in the SUS scenario, nonetheless harboring a population increase predicted by 2040. Third, in sparsely built zones an overall decrease for both scenarios can be noticed. In the SUS scenario, more than half of the current surface area has been transformed into another zone, and all small and fragmented satellite towns or villages are densified. In comparison, in the BAU scenario new sparsely built zones (LCZ 9) are created, indicating more occupation of open space. Finally, a new LCZ class, open midrise (LCZ 5), is introduced in the sustainable scenario. These zones typically sit

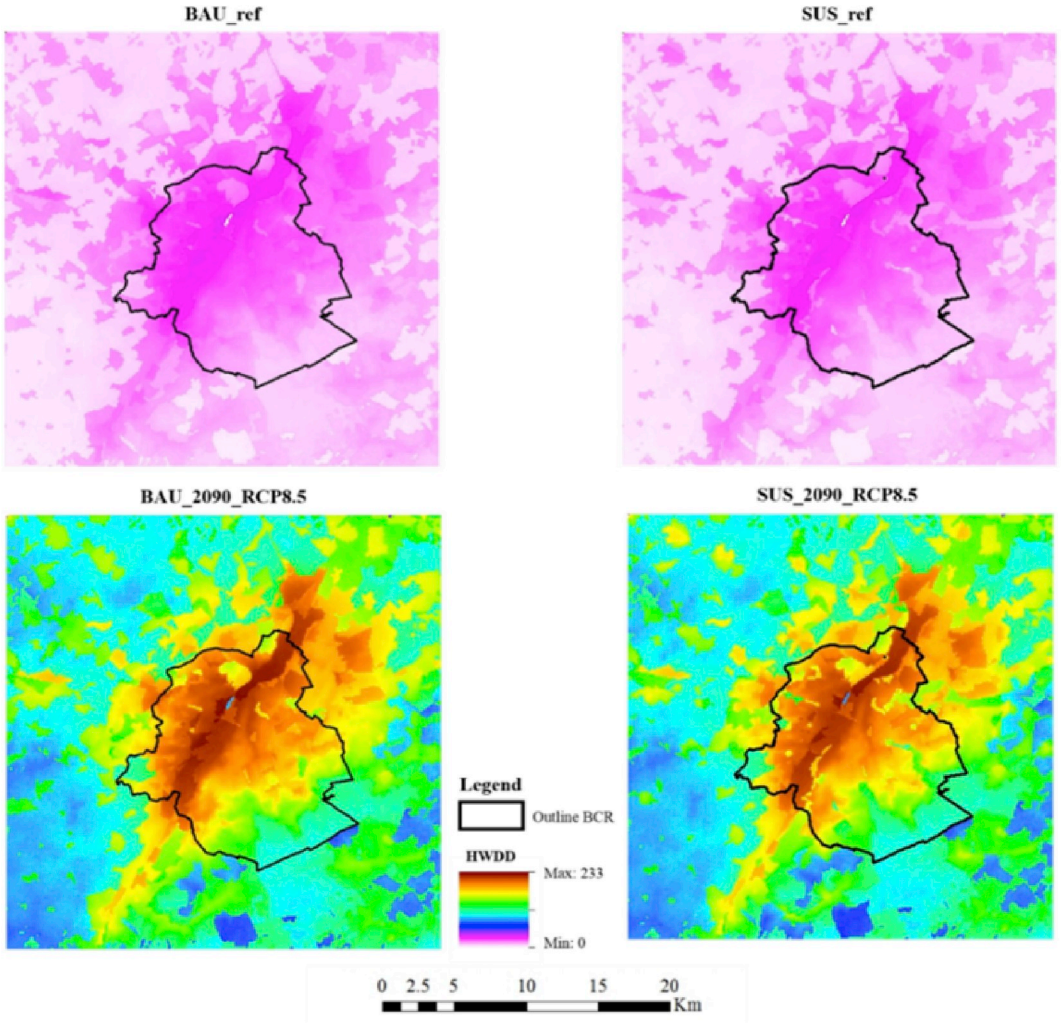

Fig. 5. Spatial explicit hazard maps for the reference period and RCP 8.5 in the far future for both UPS (BAU: left, SUS: right).

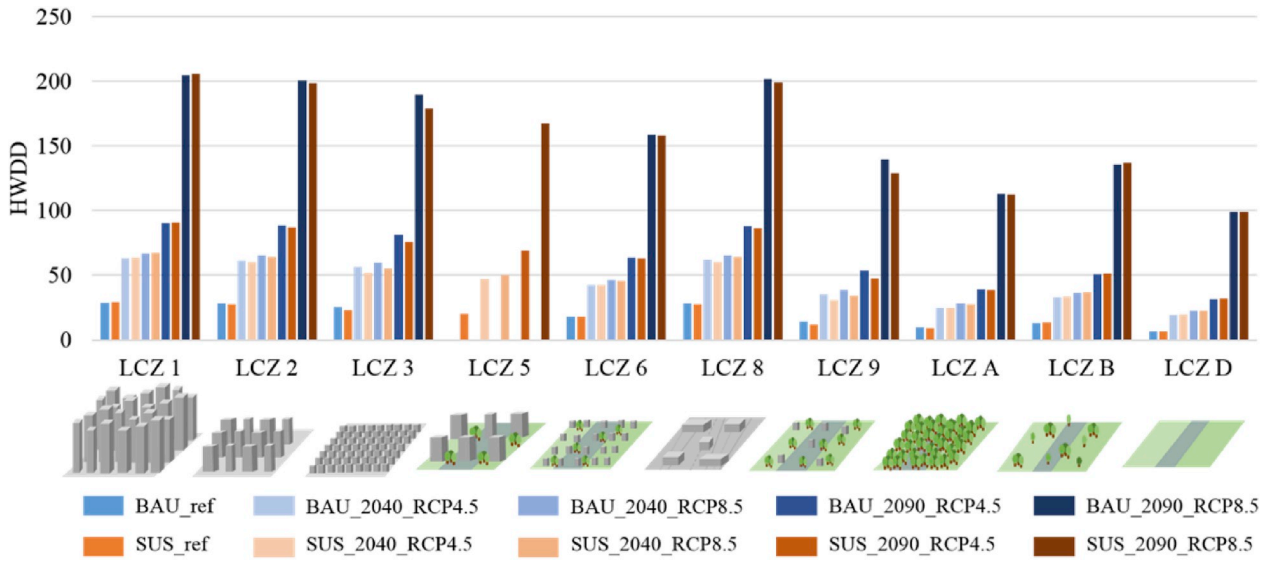

Fig. 6. Average heatwave degree days per LCZ class for all combinations of UPS and GHG scenarios (Table 3).

alongside the green corridors, likely enhancing the cool flow from the natural zones. In the sustainable scenario, the open lowrise (LCZ 6) area has decreased by 25.6 km^2 (Table 4).

3.2. Heat risk analysis in relation to LCZs

3.2.1. Hazard

Spatially explicit heatwave degree day (HWDD) maps are used as the hazard input for the heat risk analysis. In Fig. 5, the hazard maps for both the reference period and RCP 8.5 by 2090 for both UPS are shown. The same color scheme was used for all figures in Fig. 5 to ensure comparability between the periods. The maps clearly indicate that for both UPS, the Brussels Capital Region is already exposed to much higher levels of heat stress compared to the rural counterpart. Second, this figure visually shows that by 2090 under RCP 8.5 the lowest heat stress will be higher than the highest heat stress in the reference period for both UPS.

Even though Fig. 5 shows very low to low levels of heat stress under present climatic conditions, past events have shown that these areas already suffer from high levels of heat stress during heatwaves. The heat stress levels should, thus, be interpreted in comparison to the worst case scenario presented here.

Fig. 6 shows the quantification of this visual interpretation. Average HWDDs for each scenario have been calculated for each LCZ, showing a high similarity between the two urban planning scenarios in terms of HWDD for each zone (Fig. 6). For both reference periods, average HWDDs are below 30 for all zones, and the highest levels of heat stress are mainly located in the compact built and the large lowrise zones. High levels can still be found in the open built zones while medium to low values of heat stress are characteristic for sparsely built (LCZ 9) and natural zones (LCZ A, B, D). The newly introduced open midrise zone (LCZ 5) is also characterized by high heat stress levels, the levels are however lower compared to the compact zones (LCZ 1, 2, 3).

By 2040, no large differences can be seen between the UPS and the RCP scenarios, HWDDs have doubled in the hottest zones and tripled in the natural cooler zones compared to the reference period. The biggest absolute increase in heat stress is located in the built zones (Fig. 6).

By 2090, the impact caused by the RCP scenarios is bigger compared to the impact of the UPS. Under RCP 4.5, for the zones exposed to the highest levels of heat stress (compact built zones) it is now shown that heat stress values (HWDD) have tripled compared to the reference period. For the coolest zones, values are even six times higher. Under RCP 8.5, the heat stress values have doubled compared to RCP 4.5 and are almost 10 times higher compared to the reference period. The coolest zones LCZs B and D now experience the same amount of heat stress compared to the hottest compact built zones under RCP 4.5.

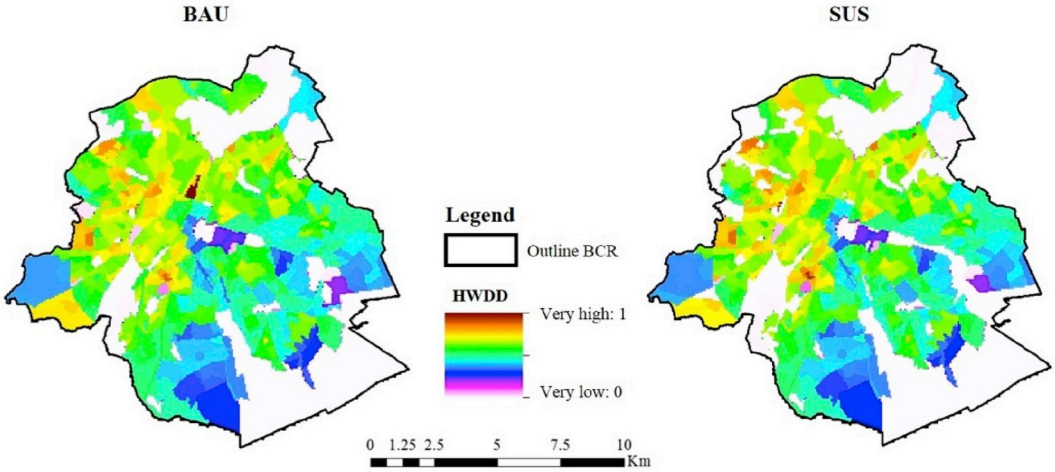

Fig. 7. Combined index for the Brussels Capital Region (BAU: left, SUS: right).

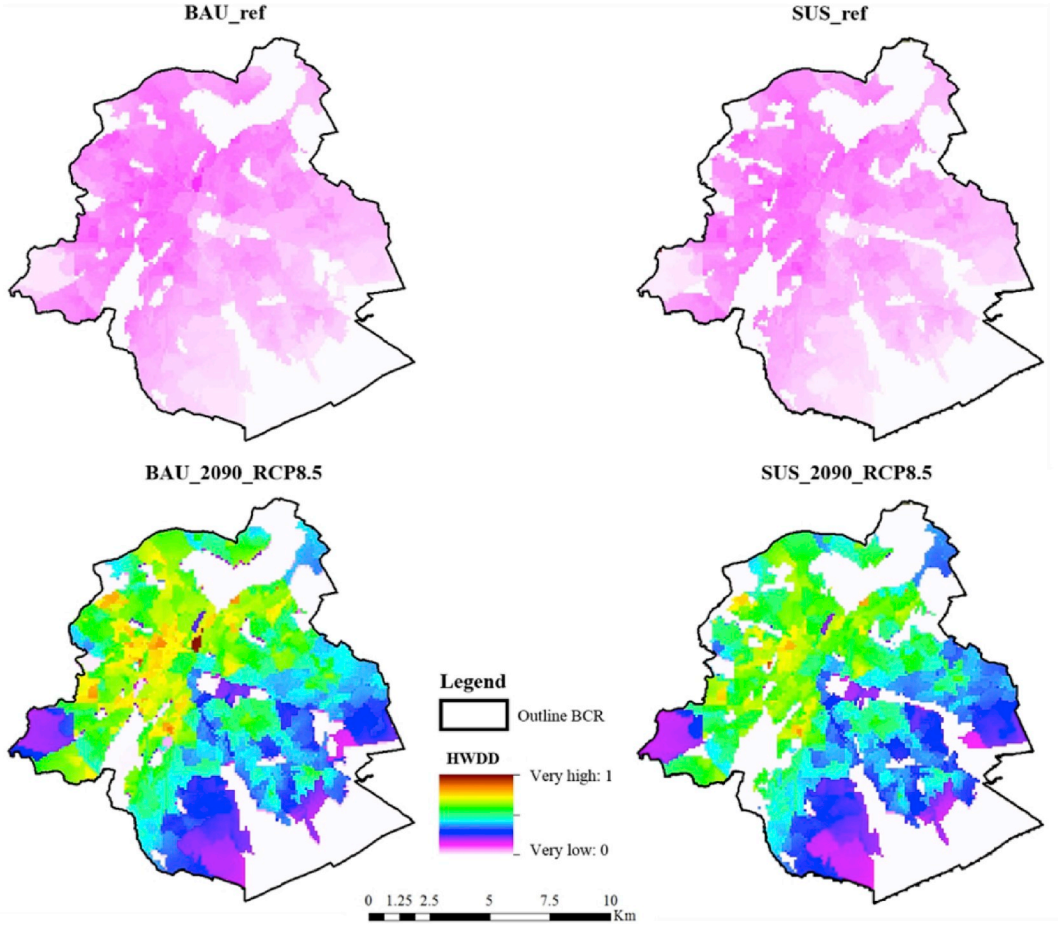

Fig. 8. Heat risk maps for the reference period and RCP 8.5 in the far future for both urban planning scenarios for the Brussels Capital Region (BAU: left, SUS: right).

3.2.2. *Exposure and vulnerability*

The combination of all normalized vulnerability indicators for both urban planning scenarios is shown in Fig. 7. Overall, the two maps do not differ much. The combined index maps show that highest vulnerability and exposure is found in the North-Western part of the city, where compact midrise dominates the built classes in both scenarios. Very low values (0 = white) are seen in the Sonian forest, the royal domain in Laken and industrial areas (e.g., neighborhood of the Brussels South railway station, elongated white area at the South-West border of the map). Very low values for the combined index are more abundant in the sustainable scenario due to the introduction of green corridors into the Brussels Capital Region.

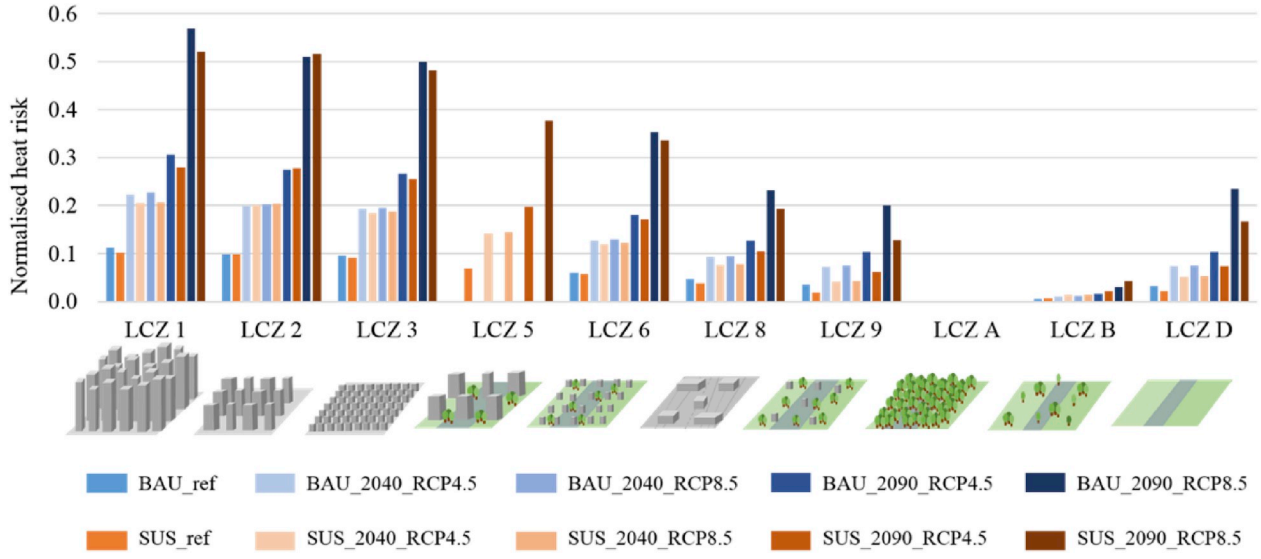

Fig. 9. Average normalized heat risk compared to the present-day heat risk (Fig. 7).

3.2.3. Risk

Similarly to heat stress, heat risk is mapped for the reference period and for RCP 8.5 by 2090, for both UPS in the Brussels Capital Region (Fig. 8). By 2090 under RCP 8.5, the results show that high to very high levels of heat risk occur for both UPS in almost the whole Brussels Capital Region, while low levels occur in the Eastern, South Eastern, and Westerns part of the Brussels Capital Region. In the SUS scenario, the green lobes clearly show and are characterized by very low heat risk (white areas). Similarly to heat stress pictured on Figs. 5 and 8 shows very low to low levels of heat risk in the whole Brussels Capital Region under present climatic conditions. These values should thus be interpreted in comparison to the worst case scenario presented here.

For each of the Local Climate Zones, the average normalized heat risk for all scenarios is presented quantitatively in Fig. 9. In 2040, the SUS scenario is exposed to slightly smaller levels of heat risk, compared to BAU for the same period. In addition, only small differences are quantified between the different RCP scenarios. The additional heat risk in the Brussels Capital Region, however, is not low: For all scenarios, heat risk has at least doubled for all LCZs. The biggest absolute increase in heat risk is seen for the built zones. In 2090, the SUS scenario is susceptible to slightly lower levels of heat risk, but large differences are found between the RCP scenarios. Heat risk is the highest under RCP 8.5, for all LCZs heat risk is five times higher compared to the reference period. The highest absolute rise in heat risk is expected in the compact built zones, dominating the Brussels Capital Region.

By 2090, it becomes clear that even though the whole Brussels Capital Region is exposed to high or very high risk, there are still large differences between the different neighborhoods. The North-Western part of the Brussels Capital Region is still the most at risk to suffer from heat stress (Fig. 8). The green corridors, introduced in the SUS scenario, are clearly visible in Figs. 7 and 8, as the population is zero, no heat risk can be present, even by 2090.

4. Discussion and conclusion

The heat risk analysis for the Brussels Capital Region indicates that the imprint of the GHG emission scenarios is much stronger compared to the different urban planning scenarios. However, they do also confirm the results of Verdonck et al. (2018) that suggest that different Local Climate Zones exhibit different thermal behavior, indicating that urban planning strategies to impact thermal comfort should not be neglected by policymakers and urban planners.

The contrasting UPS presented in this paper, translate into a different heat stress behavior. In the SUS scenario, the heat stress pattern shows high levels of heat stress surrounding mayor mobility axes and town centers. However, in this scenario a smaller surface area is subject to very high levels of heat stress in the Brussels Capital Region compared to the BAU scenario. In the BAU scenario, urban residents have to travel much larger distances to get access to zones with lower heat stress. When interpreting the maps described above one important side note should be mentioned. In Belgium, 2040) is an important date since a new policy on spatial planning will be implemented. The maps represent how a sustainable or a BAU vision could change the urban landscape in Brussels over time. Unfortunately, it should also be noted that the city and its rural counterpart might not have changed drastically by 2040. These maps provide an implementation of the current vision of space by the Belgian policymakers and should, thus, be regarded as a possibility rather than a prediction (Grimmond et al., 2011, 2010).

For both urban planning scenarios, it is clear that the Brussels city center mostly comprises compact zones. These compact zones are, however, exposed to the highest amount of heat risk. The census data in Brussels revealed that large quantities of the available surface area in the compact high and midrise zones is designated to offices or stores. Under the present situation, the most densely populated zones in Brussels are compact lowrise, which translates to two- or three-story family houses, with small city gardens or courts. Since large areas of this zone are characterized by an old and low energy efficient building stock, the compact lowrise zones show high potential for replacement by sustainable alternatives in the future (Ruimte Vlaanderen, 2016). In this respect, it is important to focus on new developments taking both mitigation (in terms of CO_2 neutral building materials, modal shift due to a changing system, smart grids, etc.) and adaptation (different urban structure, collective water retention and reuse, etc.) into account. New approaches to housing, such as co-housing and smaller private units, could offer these possibilities and ensure the livability of the city of the future. Co-housing projects in urban areas typically are designed as an open midrise zone (LCZ 5). This zone, as depicted in Fig. 6, shows lower levels of heat stress compared to compact lowrise (LCZ 6). In addition, this type of housing can house as many or more people as a compact lowrise zone and provides more green space for its inhabitants. Implementing new neighborhoods or transforming old ones into new urban structures, should, thus, be regarded as a perfect implementation of both mitigation and adaptation strategies by policymakers.

Along the lines of the results by (Wouters et al., 2017), the results in this study show that the amount of heat stress in the urban areas, by 2090, is twice as large as in their rural counterparts. The high resolution on a citywide scale not only provides information on the thermal behavior of the local climate zones, but also makes it possible to define areas prone to suffer from heat risk. The future projections show that the North-Western part of Brussels Capital Region is exposed to very high levels of heat risk. Even under RCP 8.5 by 2090, when the whole Brussels Capital Region is exposed to very high levels of heat risk, this part stands out (Fig. 8). This very high heat risk is a consequence of the high vulnerability and exposure of the population. The zones most at risk are characterized by the highest population densities in the Brussels Capital Region, a high percentage of young children and inhabitants with low incomes. Furthermore, vulnerability is difficult to predict in the future since it is influenced by exogenous factors such as conflict and poverty. This is a limitation of the study at hand; vulnerability and exposure were not projected into the future. A study by (Missirian and Schlenker, 2017) has predicted an influx of one million migrants in Europe by 2100 due to climate change, potentially increasing one of the most vulnerable population groups in Brussels. In addition, projections for Flanders and Brussels show that the fraction of people older than 65 will rise to 25% by 2030 (Pelfrene, 2005), hence, increasing this vulnerable group.

This paper asserts that unless climate change is tackled at the global level, urban areas are at risk to suffer from high levels of heat stress. Intelligent urban planning could bring solace, but the most important message is that both adaptation and mitigation strategies should be targeted on different policy levels. On the global level, it is key that countries strive to achieve the global climate deal and keep temperature rise below 2 °C. In order to achieve this, national policy should improve energy efficiency of the housing stock and industries, search for alternative ways of transportation by reducing mobilized traffic and create clear visions on urban growth to transform cities into structures with a low-carbon infrastructure and adaptation characteristics as presented in this study (Creutzig et al., 2016, 2015). Next to global mitigation and local adaptation efforts, it is important that local policymakers inform the population and induce a behavioral change at the lowest level.

This study investigated the effect of global climate on urban areas and more specifically its impact on heat risk in different LCZs. However, depending on the LCZs, not only varying GHG concentrations might be present, but also the impact of the urban environment on the global climate could be different. The latter was not part of the current research, but is definitely an interesting future research topic.

Acknowledgments

This work is funded by the Belgian Federal Science Policy Office, as part of the UrbanEARS project (SR/00/307).

Appendix A. Supplementary data

Supplementary data to this article can be found online at https://doi.org/10.1016/j.jenvman.2019.06.111.

References

Alcoforado, M.J., Andrade, H., Lopes, A., Vasconcelos, J., 2009. Application of climatic guidelines to urban planning. The example of Lisbon (Portugal). Landsc. Urban Plan. 90, 56–65. https://doi.org/10.1016/j.landurbplan.2008.10.006.

Alexander, P.J., Fealy, R., Mills, G.M., 2016. Simulating the impact of urban development pathways on the local climate: a scenario-based analysis in the greater Dublin region, Ireland. Landsc. Urban Plan. 152, 72–89. https://doi.org/10.1016/j.landurbplan.2016.02.006.

Ali, G., 2018. Climate change and associated spatial heterogeneity of Pakistan : empirical evidence using multidisciplinary approach. Sci. Total Environ. 634, 95–108. https://doi.org/10.1016/j.scitotenv.2018.03.170.

Ali, G., Pumijumnong, N., Cui, S., 2017. Decarbonization action plans using hybrid modeling for a low-carbon society: the case of Bangkok Metropolitan Area. J. Clean. Prod. 168, 940–951. https://doi.org/10.1016/j.jclepro.2017.09.049.

Ali, G., Pumijumnong, N., Cui, S., 2018. Valuation and validation of carbon sources and sinks through land cover/use change analysis: the case of Bangkok metropolitan area. Land Use Policy 70, 471–478. https://doi.org/10.1016/j.landusepol.2017.11.003.

Argüeso, D., Evans, J.P., Pitman, A.J., Luca, A. Di, 2015. Effects of city expansion on heat stress under climate change conditions. PLoS One 10, 1–19. https://doi.org/10.1371/journal.pone.0117066.

Benson-Lira, V., Georgescu, M., Kaplan, S., Vivoni, E.R., 2016. Loss of a lake system in a megacity: the impact of urban expansion on seasonal meteorology in Mexico City. J. Geophys. Res. 121, 3079–3099. https://doi.org/10.1002/2015JD024102.

BISA, 2018. Wijkmonitoring. https://wijkmonitoring.brussels/ 5.16.18.

Bramley, G., Power, S., 2009. Urban form and social sustainability: the role of density and housing type. Environ. Plan. Plan. Des. 36, 30–48. https://doi.org/10.1068/b33129.

Brouwers, J., Peeters, B., Van Steertegem, M., van Lipzig, N., Wouters, H., Beullens, J., Demuzere, M., Willems, P., De Ridder, K., Maiheu, B., De Troch, R., Termonia, P., Vansteenkiste, T., Craninx, M., Maetens, W., Defloor, W., Cauwenberghs, K., Bash, E., 2015. MIRA Klimaatrapport. VMM. https://doi.org/10.1017/CBO9781107415324.004.

Buscail, C., Upegui, E., Viel, J.F., 2012. Mapping heatwave health risk at the community level for public health action. Int. J. Health Geogr. 11, 38. https://doi.org/10.1186/1476-072X-11-38.

Chemetoff, A., 2014. Kanaalplan 02.

Creutzig, F., Baiocchi, G., Bierkandt, R., Pichler, P.-P., Seto, K.C., 2015. Global typology of urban energy use and potentials for an urbanization mitigation wedge. Proc. Natl. Acad. Sci. 112, 6283–6288. https://doi.org/10.1073/pnas.1315545112.

Creutzig, F., Agoston, P., Minx, J.C., Canadell, J.G., Andrew, R.M., Quéré, C. Le, Peters, G.P., Sharifi, A., Yamagata, Y., Dhakal, S., 2016. Urban infrastructure choices structure climate solutions. Nat. Clim. Chang. 6, 1054–1056. https://doi.org/10.1038/nclimate3169.

Crichton, D., 1999. The risk triangle. In: Ingleton, J. (Ed.), Natural Disaster Management. Tudor Rose, London, pp. 102–103.

De Ridder, K., Lauwaet, D., Maiheu, B., 2015. UrbClim - a fast urban boundary layer climate model. Urban Clim. 12, 21–48. https://doi.org/10.1016/j.uclim.2015.01.001.

Djiglav, A., 2007. People and biodiversity. In: Curitiba-Meeting, Brasil.

Dolney, T.J., Sheridan, S.C., 2006. The relationship between extreme heat and ambulance response calls for the city of Toronto, Ontario, Canada. Environ. Res. 101, 94–103. https://doi.org/10.1016/j.envres.2005.08.008.

Eliasson, I., 2000. The use of climate knowledge in urban planning. Landsc. Urban Plan. 48, 31–44.

ESPON, 2013. Small and medium sized towns in their functional territorial context. Appl. Res. 1–104.

Fischer, E.M., Oleson, K.W., Lawrence, D.M., 2012. Contrasting urban and rural heat stress responses to climate change. Geophys. Res. Lett. 39, 1–8. https://doi.org/10.1029/2011GL050576.

Gadeyne, E., 2016. Heat Stress in Citizens Exposed to Climate Change and Urbanisation (Master thesis). .

Gál, T., Lindberg, F., Unger, J., 2009. Computing continuous sky view factors using 3D urban raster and vector databases: comparison and application to urban climate. Theor. Appl. Climatol. 95, 111–123. https://doi.org/10.1007/s00704-007-0362-9.

Grimmond, C.S.B., Blackett, M., Best, M.J., Barlow, J., Baik, J.J., Belcher, S.E., Bohnenstengel, S.I., Calmet, I., Chen, F., Dandou, A., Fortuniak, K., Gouvea, M.L., Hamdi, R., Hendry, M., Kawai, T., Kawamoto, Y., Kondo, H., Krayenhoff, E.S., Lee, S.H., Loridan, T., Martilli, A., Masson, V., Miao, S., Oleson, K., Pigeon, G., Porson, A., Ryu, Y.H., Salamanca, F., Shashua-Bar, L., Steeneveld, G.J., Tombrou, M., Voogt, J., Young, D., Zhang, N., 2010. The international urban energy balance models comparison project: first results from phase 1. J. Appl. Meteorol. Climatol. 49, 1268–1292. https://doi.org/10.1175/2010JAMC2354.1.

Grimmond, C.S.B., Blackett, M., Best, M.J., Baik, J.-J., Belcher, S.E., Beringer, J., Bohnenstengel, S.I., Calmet, I., Chen, F., Coutts, A., Dandou, A., Fortuniak, K., Gouvea, M.L., Hamdi, R., Hendry, M., Kanda, M., Kawai, T., Kawamoto, Y., Kondo, H., Krayenhoff, E.S., Lee, S.-H., Loridan, T., Martilli, A., Masson, V., Miao, S., Oleson, K., Ooka, R., Pigeon, G., Porson, A., Ryu, Y.-H., Salamanca, F., Steeneveld, G.J., Tombrou, M., Voogt, J.A., Young, D.T., Zhang, N., 2011. Initial results from Phase 2 of the international urban energy balance model comparison. Int. J. Climatol. 31, 244–272. https://doi.org/10.1002/joc.2227.

Hajat, S., Kosatky, T., 2010. Heat-related mortality: a review and exploration of heterogeneity. J. Epidemiol. Community Health 64, 753–760. https://doi.org/10.1136/jech.2009.087999.

Hajat, S., Kovats, R.S., Lachowycz, K., 2007. Heat-related and cold-related deaths in england and wales: who is at risk? Occup. Environ. Med. 64, 93–100. https://doi.org/10.1136/oem.2006.029017.

Harlan, S.L., Brazel, A.J., Prashad, L., Stefanov, W.L., Larsen, L., 2006. Neighborhood microclimates and vulnerability to heat stress. Soc. Sci. Med. 63, 2847–2863. https://doi.org/10.1016/j.socscimed.2006.07.030.

Hebbert, M., Mackillop, F., 2013. Urban climatology applied to urban planning: a postwar knowledge circulation failure. Int. J. Urban Reg. Res. 37, 1542–1558. https://doi.org/10.1111/1468-2427.12046.

IPCC, 2012. Managing the Risks of Extreme Events and Disasters to Advance Climate Change Adaptation. A special report of Working Goups I and II of the IPCC. . https://doi.org/10.1017/CBO9781139177245.

Kendon, E.J., Ban, N., Roberts, N.M., Fowler, H.J., Roberts, M.J., Chan, S.C., Evans, J.P., Fosser, G., Wilkinson, J.M., 2017. Do convection-permitting regional climate models improve projections of future precipitation change? Bull. Am. Meteorol. Soc. 98, 79–93. https://doi.org/10.1175/BAMS-D-15-0004.1.

Kervyn, M., 2015. Natural Risk Management: Course Material.

Kovats, R.S., Kristie, L.E., 2006. Heatwaves and public health in Europe. Eur. J. Public Health 16, 592–599. https://doi.org/10.1093/eurpub/ckl049.

Lemonsu, A., Viguié, V., Daniel, M., Masson, V., 2015. Vulnerability to heat waves: impact of urban expansion scenarios on urban heat island and heat stress in Paris (France). Urban Clim. 14, 586–605. https://doi.org/10.1016/j.uclim.2015.10.007.

Loughnan, M., Nicholls, N., Tapper, N.J., 2012. Mapping heat health risks in urban areas. Int. J. Popul. Res. 2012, 1–12. https://doi.org/10.1155/2012/518687.

Luber, G., McGeehin, M., 2008. Climate change and extreme heat events. Am. J. Prev. Med. 35, 429–435. https://doi.org/10.1016/j.amepre.2008.08.021.

Mills, G., 2007. Cities as agents of global change. Int. J. Climatol. 27, 1849–1857. https://doi.org/10.1002/joc.

Mills, G., Cleugh, H., Emmanuel, R., Endlicher, W., Erell, E., McGranahan, G., Ng, E., Nickson, A., Rosenthal, J., Steemer, K., 2010. Climate information for improved planning and management of mega cities (Needs Perspective). Procedia Environ. Sci. 1, 228–246. https://doi.org/10.1016/j.proenv.2010.09.015.

Missirian, A., Schlenker, W., 2017. Asylum applications respond to temperature fluctuations. Science 358 (80), 1610–1614. https://doi.org/10.1126/science.aao0432.

Morabito, M., Crisci, A., Gioli, B., Gualtieri, G., Toscano, P., Di Stefano, V., Orlandini, S., Gensini, G.F., 2015. Urban-hazard risk analysis: mapping of heat-related risks in the elderly in major Italian cities. PLoS One 10, 1–18. https://doi.org/10.1371/journal.pone.0127277.

Oleson, K.W., Anderson, G.B., Jones, B., McGinnis, S.A., Sanderson, B., 2018. Avoided climate impacts of urban and rural heat and cold waves over the U.S. using large climate model ensembles for RCP8.5 and RCP4.5. Clim. Change 146, 377–392. https://doi.org/10.1007/s10584-015-1504-1.

Pelfrene, E., 2005. Ontgroening en vergrijzing in Vlaanderen 1990-2050: Verkenningen op basis van de NIS-bevolkingsvooruitzichten.

Poelmans, L., 2010. Modelling Urban Expansion and its Hydrological Impacts (Phd dissertation). .

Revi, A., Satterthwaite, D.E., Aragón-Durand, F., Corfee-Morlot, J., Kiunsi, R.B.R., Pelling, M., Roberts, D.C., Solecki, W., 2014. Urban areas. In: Field, C.B. (Ed.), Climate Change 2014: Impacts, Adaptation, and Vulnerability. Part A: Global and Sectoral Aspects. Contribution of Working Group II to the Fifth Assessment Report of the Intergovernmental Panel on Climate Change. Cambridge University Press, Cambridge, U.K. and New Tork, pp. 535–612.

Ruimte Vlaanderen, 2016. Witboek: Beleidsplan Ruimte Vlaanderen. Bema Graphics.

Scheraga, J., Grambsch, A., 1998. Risks, opportunities and adaptation to climate change. Clim. Res. 11, 85–95. https://doi.org/10.3354/cr011085.

Scherer, D., Fehrenbach, U., Lakes, T., Lauf, S., Meier, F., Schuster, C., 2013. Quantification of heat-Stress related mortality hazard, vulnerability and risk in Berlin, Germany. Erde 144, 238–259. https://doi.org/10.12854/erde-144-17.

Seto, K.C., Güneralp, B., Hutyra, L.R., 2012. Global forecasts of urban expansion to 2030 and direct impacts on biodiversity and carbon pools. Proceedings of the National Academy of Sciences of the United States of America 109 (40), 16083–16088. https://doi.org/10.1073/pnas.1211658109.

Somers, B., Canters, F., Van Coillie, F., Demuzere, M., Verbeiren, B., Degericks, J., Priem, F., M.L., V., Wirion, C., 2017. Activity Report: Urban Ecosysem Analysis Supported by Remote Sensing.

Stewart, I.D., Oke, T.R., 2012. Local climate zones for urban temperature studies. Bull. Am. Meteorol. Soc. 93, 1879–1900. https://doi.org/10.1175/BAMS-D-11-00019.1.

Stewart, I.D., Oke, T.R., Krayenhoff, E.S., 2014. Evaluation of the “local climate zone” scheme using temperature observations and model simulations. Int. J. Climatol. 34, 1062–1080. https://doi.org/10.1002/joc.3746.

Tomlinson, C.J., Chapman, L., Thornes, J.E., Baker, C.J., 2011. Including the urban heat island in spatial heat health risk assessment strategies: a case study for Birmingham, UK. Int. J. Health Geogr. 10, 42. https://doi.org/10.1186/1476-072X-10-42.

Van De Voorde, T., Van Der Kwast, J., Poelmans, L., Canters, F., Binard, M., Cornet, Y., Engelen, G., Uljee, I., Shahumyan, H., Williams, B., Convery, S., Lavalle, C., 2016. Projecting alternative urban growth patterns: the development and application of a remote sensing assisted calibration framework for the greater Dublin area. Ecol. Indicat. 60, 1056–1069. https://doi.org/10.1016/j.ecolind.2015.08.035.

Vandentorren, S., Bretin, P., Zeghnoun, A., Mandereau-Bruno, L., Croisier, A., Cochet, C., Ribéron, J., Siberan, I., Declercq, B., Ledrans, M., 2006. August 2003 heat wave in France: risk factors for death of elderly people living at home. Eur. J. Public Health 16, 583–591. https://doi.org/10.1093/eurpub/ckl063.

Verdonck, M.L., Okujeni, A., van der Linden, S., Demuzere, M., De Wulf, R., Van Coillie, F., 2017. Influence of neighbourhood information on ' Local Climate Zone ' mapping in heterogeneous cities. Int. J. Appl. Earth Obs. Geoinf. 62, 102–113. https://doi.org/10.1016/j.jag.2017.05.017.

Verdonck, M.L., Demuzere, M., Hooyberghs, H., Beck, C., Cyrys, J., Schneider, A., Dewulf, R., Van Coillie, F., 2018. The potential of local climate zones maps as a heat stress assessment tool, supported by simulated air temperature data. Landsc. Urban Plan. 178, 183–197. https://doi.org/10.1016/j.landurbplan.2018.06.004.

Watts, N., Adger, W.N., Agnolucci, P., 2015. Changement climatique: agir au nom de la santé publique. Environnement, Risques & Santé 14, 466–468. https://doi.org/10.1016/S0140-6736(15)60854-6.

White, R., Engelen, G., 2000. High-resolution integrated modelling of the spatial dynamics of urban and regional systems. Comput. Environ. Urban Syst. 24, 383–400. https://doi.org/10.1016/S0198-9715(00)00012-0.

Wisner, B., Blaikie, P., Cannon, T., Davis, I., 2003. At Risk: Natural Hazards, People's Vulnerability, and Disasters. Routledge, New York/London. https://doi.org/10.2202/1547-7355.1131.

WMO, WHO, 2015. Heatwaves and Health: Guidance on Warning-System Development.

Wouters, H., De Ridder, K., Poelmans, L., Willems, P., Brouwers, J., Hosseinzadehtalaei, P., Tabari, H., Vanden Broucke, S., van Lipzig, N.P.M., Demuzere, M., 2017. Heat stress increase under climate change twice as large in cities as in rural areas: a study for a densely populated midlatitude maritime region. Geophys. Res. Lett. 44, 8997–9007. https://doi.org/10.1002/2017GL074889.